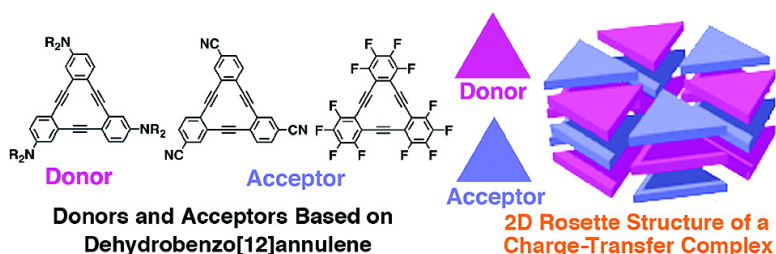


## Donors and Acceptors Based on Triangular Dehydrobenzo[12]annulenes: Formation of a Triple-Layered Rosette Structure by a Charge-Transfer Complex

Kazukuni Tahara, Takumi Fujita, Motohiro Sonoda, Motoo Shiro, and Yoshito Tobe

*J. Am. Chem. Soc.*, **2008**, 130 (43), 14339-14345 • DOI: 10.1021/ja804604y • Publication Date (Web): 25 September 2008

Downloaded from <http://pubs.acs.org> on February 8, 2009



### More About This Article

Additional resources and features associated with this article are available within the HTML version:

- Supporting Information
- Links to the 2 articles that cite this article, as of the time of this article download
- Access to high resolution figures
- Links to articles and content related to this article
- Copyright permission to reproduce figures and/or text from this article

[View the Full Text HTML](#)

## Donors and Acceptors Based on Triangular Dehydrobenzo[12]annulenes: Formation of a Triple-Layered Rosette Structure by a Charge-Transfer Complex

Kazukuni Tahara,<sup>†</sup> Takumi Fujita,<sup>†</sup> Motohiro Sonoda,<sup>†,§</sup> Motoo Shiro,<sup>‡</sup> and Yoshito Tobe<sup>\*,†</sup>

*Division of Frontier Materials Science, Graduate School of Engineering Science, Osaka University, Toyonaka, Osaka 560-8531, Japan, and Rigaku Corporation, 3-9-12 Matsubaracho, Akishima, Tokyo 196-8666, Japan*

Received June 17, 2008; E-mail: tobe@chem.es.osaka-u.ac.jp

**Abstract:** We present here the results of studies of the synthesis and properties of donors and acceptors based on triangular dehydrobenzo[12]annulene ([12]DBA) system as a  $\pi$  core. These studies were aimed at controlling the supramolecular crystal structure. Toward this end, the tricyano[12]DBA **2** and dodecafluoro[12]DBA (**3**) were synthesized as acceptors (A) and the tris(dialkylamino)[12]DBAs **4a–d** as donors (D), and their electronic properties were determined by electronic absorption spectroscopy and electrochemical measurements. The main focus, though, was the formation of supramolecular structures in crystals. These compounds form distinct packing patterns as a result of the different intermolecular interactions. Tricyano[12]DBA **2** forms a two-dimensional (2D) sheet structure via hydrogen-bonding interactions, whereas a tilted-stack structure was found for **3** because of the lack of significant intermolecular interactions. Tris(dibutylamino)[12]DBA **4b** exhibits a ladder-type 2D structure, probably because of van der Waals interactions between the butyl groups. The most significant finding is that charge-transfer interactions between donor **4a** and acceptor **3** combined with their triangular molecular shapes and lateral CH $\cdots$ F hydrogen bonding result in the formation of a 2D rosette structure consisting of two different trimeric (DAD- and ADA-type) sandwich structures with 1:2 and 2:1 A/D ratios, respectively.

### Introduction

Engineering the self-assembly of  $\pi$ -conjugated molecules into well-defined nanometer-scale structures by controlling intermolecular noncovalent interactions<sup>1</sup> has led to major advances in the production of novel materials, such as porous crystals for gas storage,<sup>2</sup> liquid-crystalline materials,<sup>3</sup> and gel or sol materials.<sup>4</sup> The first step in achieving a highly ordered nanostructure is to investigate the correlation of the molecular features, such as directional intermolecular interactions originating from the functionality and electronic properties as well as the intrinsic molecular shape, with the resulting topology of the self-assembled architectures. Through the use of this

approach, numerous superstructures with unique topologies have been constructed.<sup>1–6</sup>

Despite their ability to exhibit unique assemblies such as hexagonal close packing, molecules with threefold symmetry have not been fully investigated because of the limited number of known compounds having  $\pi$  cores. Triphenylene derivatives with tuned intermolecular forces and electronic properties show various intriguing properties, such as formation of one-dimensional (1D) columnar assembly,<sup>3,7</sup> hole-transport properties in the column,<sup>8</sup> and formation of charge-transfer complexes with a triplet ground state.<sup>9</sup> Formal expansion of the triphenylene

<sup>†</sup> Osaka University.

<sup>‡</sup> Rigaku Corporation.

<sup>§</sup> Present address: Department of Applied Chemistry, Graduate School of Engineering, Osaka Prefecture University, Japan.

- (1) (a) Hoeben, F. J. M.; Jonkheijm, P.; Meijer, E. W.; Schenning, A. P. H. J. *Chem. Rev.* **2005**, *105*, 1491–1546. (b) Grimsdale, A. C.; Müllen, K. *Angew. Chem., Int. Ed.* **2005**, *44*, 5592–5629.
- (2) (a) Eddaoudi, M.; Kim, J.; Rosi, N.; Vodak, D.; Wachter, J.; O’Keeffe, M.; Yagi, O. M. *Science* **2002**, *295*, 469–472. (b) Zhao, X.; Xiao, B.; Fletcher, A. J.; Thomas, K. M.; Bradshaw, D.; Rosseinsky, M. J. *Science* **2008**, *306*, 1012–1015. (c) Matsuda, R.; Kitaura, R.; Kitagawa, S.; Kubota, Y.; Belosludov, R. V.; Kobayashi, T. C.; Sakamoto, H.; Chiba, T.; Takata, M.; Kawazoe, Y.; Mita, Y. *Nature* **2005**, *436*, 238–241.
- (3) Laschat, S.; Baro, A.; Steinke, N.; Giesselmann, F.; Hägele, C.; Scalia, G.; Judele, R.; Kapatsina, E.; Sauer, S.; Schreivogel, A.; Tosoni, M. *Angew. Chem., Int. Ed.* **2007**, *46*, 4832–4887.
- (4) Terech, P.; Weiss, R. G. *Chem. Rev.* **1997**, *97*, 3133–3160.

- (5) (a) Schmidt, G. M. J. *Pure Appl. Chem.* **1971**, *27*, 647–678. (b) *Crystal Engineering: The Design of Organic Solids*; Desiraju, G. R., Ed.; Elsevier: Amsterdam, 1989. (c) Desiraju, G. R. *Angew. Chem., Int. Ed. Engl.* **1995**, *34*, 2311–2327. (d) Blagden, N.; Davey, R. J. *Cryst. Growth Des.* **2003**, *3*, 873–885.
- (6) (a) Barth, J. V. *Amu. Rev. Phys. Chem.* **2007**, *58*, 375–407 (b) Furukawa, S.; De Feyter, S. *Top. Curr. Chem.*, DOI 10.1007/128\_2008\_6.
- (7) (a) Malthete, J.; Destrade, C.; Tinh, N. H.; Jacques, J. *Mol. Cryst. Liq. Cryst. Lett.* **1981**, *64*, 233–238. (b) Destrade, C.; Nguyen, H. T.; Gasparoux, H.; Malthete, J.; Levelut, A. M. *Mol. Cryst. Liq. Cryst.* **1981**, *71*, 111–114.
- (8) (a) Adam, D.; Schuhmacher, P.; Simmerer, J.; Häußling, L.; Paulus, W.; Siemensmeyer, K.; Etzbach, K.-H.; Ringsdorf, H.; Haarer, D. *Adv. Mater.* **1995**, *7*, 276–280. (b) Adam, D.; Schuhmacher, P.; Simmerer, J.; Häußling, L.; Siemensmeyer, K.; Etzbach, K. H.; Ringsdorf, H.; Haarer, D. *Nature* **1994**, *371*, 141–143.
- (9) (a) Breslow, R.; Jaun, B.; Kluttz, R. Q.; Xia, C.-Z. *Tetrahedron* **1982**, *38*, 863–867. (b) LePage, T. J.; Breslow, R. *J. Am. Chem. Soc.* **1987**, *109*, 6412–6421.

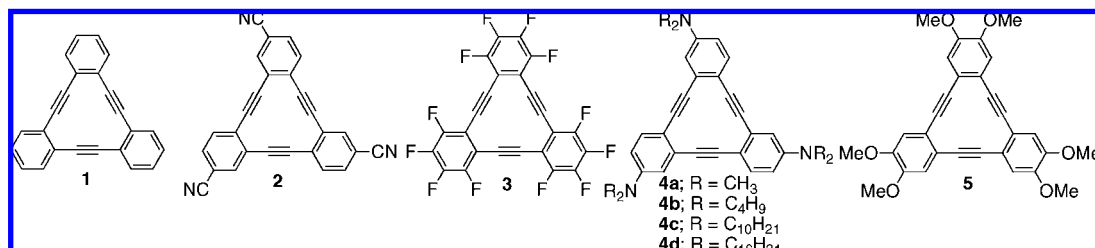


**Figure 1.** Chemical structures of the parent molecule [12]DBA (**1**) and [12]DBAs functionalized with electron-withdrawing groups (the tricyano[12]DBA **2** and dodecafluoro[12]DBA **3**) and with electron-donating groups (the tris(dialkylamino)[12]DBAs **4a–d** and hexamethoxy[12]DBA **5**).

conjugation with the trigonal shape by benzoannulation leads to a nanographene system,<sup>10</sup> but insertion of triple bonds leads to dehydrobenzo[12]annulene ([12]DBA)<sup>11</sup> and dehydrobenzo[18]annulene ([18]DBA),<sup>12</sup> which consist of weakly antiaromatic 12-membered and aromatic 18-membered rings, respectively, that are stabilized by the three fused aromatic rings.<sup>13</sup> Contrary to the triphenylene and [18]DBA<sup>14,15</sup> systems, little has been done with respect to systematic electronic modulation of the [12]DBA  $\pi$  system,<sup>11d</sup> though [12]DBAs have currently become subjects of interest in supramolecular chemistry involving formation of liquid crystals,<sup>17</sup> vesicles,<sup>18</sup> and two-dimensional (2D) molecular networks at solid–liquid interfaces.<sup>19</sup> Therefore, there is plenty of room to create novel materials utilizing the assembly of appropriately functionalized triangular [12]DBAs.

One of the intriguing molecular assemblies based on a  $C_3$ -symmetric trigonal molecular unit is a bimolecular rosette.

Whitesides and co-workers<sup>20</sup> proposed the rosette structure consisting of cyanuric acid and melamine and performed pioneering work on the formation of supramolecular complexes between derivatives of these compounds. Later on, Rao and co-workers confirmed the formation of the 2D rosette structure in a crystal prepared by a hydrothermal synthesis.<sup>21</sup> Since then, rosette units have been employed for the construction of many supramolecular assemblies, such as a tubular assembly<sup>22</sup> and a monolayer on a surface.<sup>23</sup>

Motivated by the possible formation of supramolecular assemblies that reflect the unique  $C_3$ -symmetric structure of the [12]DBA core, we planned to prepare electronically tuned [12]DBAs. Toward this end, we designed [12]DBAs substituted with electron-donating groups (such as the tris(dialkylamino)[12]DBAs **4a–d**) or electron-withdrawing groups (such as tricyano[12]DBA **2** and dodecafluoro[12]DBA **3**) (Figure 1). We expected that the supramolecular structures would be affected by not only charge transfer but also specific intermolecular interactions between the functional groups. Analysis of the superstructures in crystals of **2**, **3**, and **4b** revealed that they form distinct packing structures: a perfect 2D sheet structure for **2**, a tilted-stack structure for **3**, and a ladder-type 2D structure for **4b**, depending on the features of the functionalities. Moreover, we found that a 1:1 charge-transfer complex between **3** and **4a** formed a 2D triple-layered rosette structure consisting of two different trimeric molecular sandwiches containing **3** and **4a** in 2:1 and 1:2 ratios. The two trimers together with two

- (10) (a) Feng, X.; Wu, J.; Ai, M.; Pisula, W.; Zhi, L.; Rabe, J. P.; Müllen, K. *Angew. Chem., Int. Ed.* **2007**, *46*, 3033–3036. (b) Fujioka, Y. *Bull. Chem. Soc. Jpn.* **1985**, *58*, 481–489.
- (11) (a) Campbell, I. D.; Eglinton, G.; Henderson, W.; Raphael, R. A. *Chem. Commun.* **1996**, 87–89. (b) Staab, H. A.; Graf, F. *Tetrahedron Lett.* **1966**, *7*, 751–757. (c) Huynh, C.; Linstremelle, G. *Tetrahedron* **1988**, *44*, 6337–6344. (d) Iyoda, M.; Vorasingha, A.; Kuwatani, Y.; Yoshida, M. *Tetrahedron Lett.* **1998**, *39*, 4701–4704. (e) Iyoda, M.; Sirinintasak, S.; Nishiyama, Y.; Vorasingha, A.; Sultana, F.; Nakao, K.; Kuwatani, Y.; Matsuyama, H.; Yoshida, M.; Miyake, Y. *Synthesis* **2004**, 1527–1531. (f) Kehoe, J. M.; Kiley, J. H.; English, J. J.; Johnson, C. A.; Peterson, R. C.; Haley, M. M. *Org. Lett.* **2000**, *2*, 969–972.
- (12) (a) Behr, O. M.; Eglinton, G.; Galbraith, A. R.; Raphael, R. A. *J. Chem. Soc.* **1960**, 3614–3625. (b) Haley, M. M.; Brand, S. C.; Pak, J. J. *Angew. Chem., Int. Ed. Engl.* **1997**, *36*, 836–838. (c) Wan, W. B.; Brand, S. C.; Pak, J. J.; Haley, M. M. *Chem.–Eur. J.* **2000**, *6*, 2044–2052.
- (13) For recent reviews on dehydrobenzoannulenes, see: (a) Youngs, W. J.; Tessier, C. A.; Bradshaw, J. D. *Chem. Rev.* **1999**, *99*, 3153–3180. (b) Spitler, E. L.; Johnson, C. A.; Haley, M. M. *Chem. Rev.* **2006**, *106*, 5344–5386. (c) Tobe, Y.; Sonoda, M. In *Modern Cyclophane Chemistry*; Gleiter, R.; Hopf, H., Eds.; Wiley-VCH: Weinheim, Germany, 2004; pp 1–40. (d) Jones, C. S.; O'Connor, M. J.; Haley, M. M. In *Acetylene Chemistry: Chemistry, Biology and Material Science*; Diederich, F.; Stang, P. J.; Tykwinski, R. R., Eds.; Wiley-VCH: Weinheim, Germany, 2005; pp 303–385.
- (14) (a) Zhou, Q.; Carroll, P. J.; Swager, T. M. *J. Org. Chem.* **1994**, *59*, 1294–1301. (b) Nishinaga, T.; Nodera, N.; Miyata, Y.; Komatsu, K. *J. Org. Chem.* **2002**, *67*, 6091–6096. (c) Nishinaga, T.; Miyata, Y.; Nodera, N.; Komatsu, K. *Tetrahedron* **2004**, *60*, 3375–3382. (d) Pak, J. J.; Weakley, T. J. R.; Haley, M. M. *J. Am. Chem. Soc.* **1999**, *121*, 8182–8192. (e) Sarkar, A.; Pak, J. J.; Rayfield, G. W.; Haley, M. M. *J. Mater. Chem.* **2001**, *11*, 2943–2945. (f) Tahara, K.; Johnson, C. A.; Fujita, T.; Sonoda, M.; De Schryver, F. C.; De Feyter, S.; Haley, M. M.; Tobe, Y. *Langmuir* **2007**, *23*, 10190–10197. (g) Zhou, X.; Ren, A.-M.; Feng, J.-K.; Liu, X.-J. *Can. J. Chem.* **2004**, *82*, 1172–1178.
- (15) For similar electronic modulation in dehydrobenzo[14]annulene  $\pi$ -systems, see: (a) Marsden, J. A.; Miller, J. J.; Haley, M. M. *Angew. Chem., Int. Ed.* **2004**, *43*, 1694–1697. (b) Marsden, J. A.; Miller, J. J.; Shirtcliff, L. D.; Haley, M. M. *J. Am. Chem. Soc.* **2005**, *127*, 2464–2476. (c) Spitler, E. L.; Monson, J. M.; Haley, M. M. *J. Org. Chem.* **2008**, *73*, 2211–2223.

- (16) (a) Kinder, J. D.; Tessier, C. A.; Youngs, W. J. *Synlett* **1993**, 149–150. (b) Miljanić, O. Š.; Vollhardt, K. P. C.; Whitener, G. D. *Synlett* **2003**, 29–34. (c) Li, Y.; Zhang, J.; Wang, W.; Miao, Q.; She, X.; Pan, X. *J. Org. Chem.* **2005**, *70*, 3285–3287. (d) Zhang, W.; Brombosz, S. M.; Mendoza, J. L.; Moore, J. S. *J. Org. Chem.* **2005**, *70*, 10198–10201.
- (17) Seo, S. H.; Jones, T. V.; Seyler, H.; Peters, J. O.; Kim, T. H.; Chang, J. Y.; Tew, G. N. *J. Am. Chem. Soc.* **2006**, *128*, 9264–9265.
- (18) Seo, S. H.; Chang, J. Y.; Tew, G. N. *Angew. Chem., Int. Ed.* **2006**, *45*, 7526–7530.
- (19) (a) Furukawa, S.; Uji-i, H.; Tahara, K.; Ichikawa, T.; Sonoda, M.; De Schryver, F. C.; Tobe, Y.; De Feyter, S. *J. Am. Chem. Soc.* **2006**, *128*, 3502–3503. (b) Tahara, K.; Furukawa, S.; Uji-i, H.; Uchino, T.; Ichikawa, T.; Zhang, J.; Sonoda, M.; De Schryver, F. C.; De Feyter, S.; Tobe, Y. *J. Am. Chem. Soc.* **2006**, *128*, 16613–16625. (c) Lei, S.; Tahara, K.; De Schryver, F. C.; Van der Auweraer, M.; Tobe, Y.; De Feyter, S. *Angew. Chem., Int. Ed.* **2008**, *47*, 2964–2968. (d) Furukawa, S.; Tahara, K.; De Schryver, F. C.; Van der Auweraer, M.; Tobe, Y.; De Feyter, S. *Angew. Chem., Int. Ed.* **2007**, *46*, 2831–2834. (e) Lei, S.; Tahara, K.; Feng, X.; Furukawa, S.; De Schryver, F. C.; Müllen, K.; Tobe, Y.; De Feyter, S. *J. Am. Chem. Soc.* **2008**, *130*, 7119–7129. (f) Tahara, K.; Lei, S.; Mössinger, D.; Kozuma, H.; Inukai, K.; Van der Auweraer, M.; De Schryver, F. C.; Höger, S.; Tobe, Y.; De Feyter, S. *Chem. Commun.* **2008**, 3897–3899.
- (20) (a) Seto, C. T.; Whitesides, G. M. *J. Am. Chem. Soc.* **1991**, *113*, 712–713. (b) Seto, C. T.; Whitesides, G. M. *J. Am. Chem. Soc.* **1993**, *115*, 905–916. (c) Whitesides, G. M.; Simanek, E. E.; Mathias, J. P.; Seto, C. T.; Chin, D.; Mammen, M.; Gordon, D. M. *Acc. Chem. Res.* **1995**, *28*, 37–44. (d) Whitesides, G. M.; Mathias, J. P.; Seto, C. T. *Science* **1991**, *254*, 1312–1319.

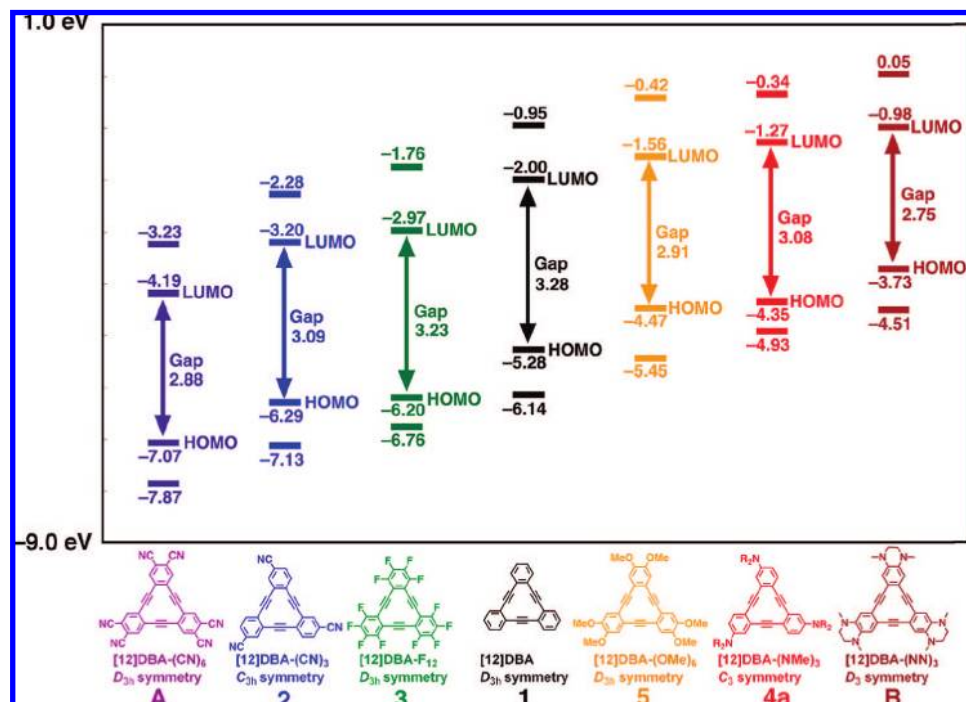


**Figure 2.** HOMO-1, HOMO, LUMO, and LUMO+1 energy levels (eV) and the HOMO–LUMO gaps (eV) obtained from DFT calculations on the [12]DBAs 1–3, 4a, 5, A, and B at B3LYP/6-31G\* level of theory.

chloroform molecules constitute the repeating units, and they align alternately in forming the triple-layered rosette structure. To the best of our knowledge, this is the first example of the formation of a 2D bimolecular rosette by triangular-shaped molecules.

## Results and Discussion

**1. Molecular Design and Syntheses.** To predict the effect of the functional groups on the  $\pi$ -electron systems of the [12]DBAs, density functional theory (DFT) calculations at the B3LYP/6-31G\* level for **1**, **2**, **3**, **4a**, **5**, the hexacyano[12]DBA **A**, and the tris(*N,N*-dimethyltetrahydropyrazino)[12]DBA **B** were performed, and the energy levels of their frontier molecular orbitals (MOs) were computed. The HOMO-1, HOMO, LUMO, and LUMO+1 levels are summarized in Figure 2. Molecules **A**, **2**, and **3** are acceptors; their HOMO and LUMO levels, respectively, are located at  $-7.07$  and  $-4.19$  eV for **A**,  $-6.29$  and  $-3.20$  eV for **2**, and  $-6.20$  and  $-2.97$  eV for **3**. Not surprisingly, both levels of each acceptor are lower than the corresponding levels of the parent **1** ( $-5.28$  and  $-2.00$  eV) as a result of the electron-accepting ability of the substituents. In addition, as far as the MO levels are concerned, it appears that cyano groups enhance the electron-acceptability of the [12]DBA system more efficiently than fluoro groups. On the other hand, the HOMO and LUMO levels, respectively, of the donors **4a**, **B**, and **5** ( $-4.35$  and  $-1.27$  eV for **4a**, and  $-3.73$  and  $-0.98$  eV for **B**, and  $-4.47$  and  $-1.56$  eV for **5**) are higher than the corresponding levels

of **1**, again as expected. Notably, introducing three amino groups (as in **4a**) enhances the electron-donating ability better than introducing six methoxy groups (as in **5**).

For comparison, the energy levels of the triphenylene derivatives having the same functional groups were computed. All of the triphenylene compounds possess lower HOMO and higher LUMO energies (e.g.,  $-5.82$  and  $-0.93$  eV for parent triphenylene,  $-7.05$  and  $-2.52$  eV for the tricyanotriphenylene, and  $-4.76$  and  $-0.42$  eV for the tris(dimethylamino)triphenylene; see Figure S1 in the Supporting Information) than the corresponding [12]DBA derivatives as a result of the reduced  $\pi$  conjugation.

Though the theoretical study predicted that the model compounds **A** and **B** would be the most efficient acceptor and donor, respectively, in view of obstacles that we met in the synthesis of **2** (i.e., low solubility in common organic solvents) and in our attempts to prepare a suitable precursor of **B** (i.e., via halogenation of *N,N*-dimethyltetrahydroquinoxaline by an electrophilic substitution reaction), we decided to focus on **2** and **3** as acceptors and **4a–d** as donors.

The [12]DBAs **2**, **3**, and **4a–d** were synthesized by the cyclotrimerization reactions of the corresponding *o*-ethynyliodobenzene derivatives under two different conditions, the Sonogashira–Hagihara-type reaction for **2** and **3** and the Stephens–Castro-type reaction for **4a–d**, in view of the threefold-symmetric nature of the target molecules and minimization of the number of synthetic steps. Absorption and fluorescence spectra of **2**, **3**, **4a**, and **5** are qualitatively in accord with the theoretical predictions for their MO levels. Details of the syntheses of **2**, **3**, and **4a–d** and electronic absorption and emission spectra of **1–3**, **4a–d**, and **5** are provided in the Supporting Information.

**2. Electrochemical Measurements.** Electrochemical measurement is a powerful tool for investigating the electronic properties

- (21) Ranganathan, A.; Pedireddi, V. R.; Rao, C. N. R. *J. Am. Chem. Soc.* **1999**, *121*, 1752–1753.  
 (22) Yagai, S.; Nakajima, T.; Kishikawa, K.; Kohmoto, S.; Karatsu, T.; Kitamura, A. *J. Am. Chem. Soc.* **2005**, *127*, 11134–11139.  
 (23) Schönherr, H.; Paraschiv, V.; Zapotoczny, S.; Crego-Calama, M.; Timmerman, P.; Frank, C. W.; Vancso, G. J.; Reinhoudt, D. N. *Proc. Natl. Acad. Sci. U.S.A.* **2002**, *99*, 5024–5027.

**Table 1.** Results of Cyclic Voltammetry Measurements on [12]DBAs<sup>a</sup>

compound	solvent	$E_{1/2}(\text{red})$ (V) <sup>b</sup>	$E_{\text{pa}}(\text{ox 1})$ (V) <sup>b</sup>	$E_{\text{pa}}(\text{ox 2})$ (V) <sup>b</sup>
<b>1</b>	CH <sub>2</sub> Cl <sub>2</sub>	-2.21	— <sup>d</sup>	— <sup>d</sup>
<b>2</b>	C <sub>2</sub> H <sub>2</sub> Cl <sub>4</sub>	-1.70	— <sup>d</sup>	— <sup>d</sup>
<b>3</b>	C <sub>2</sub> H <sub>2</sub> Cl <sub>4</sub>	-1.70	— <sup>d</sup>	— <sup>d</sup>
<b>4a</b>	CH <sub>2</sub> Cl <sub>2</sub>	— <sup>e</sup>	0.30 <sup>c</sup>	0.61 <sup>c</sup>
<b>5</b>	CH <sub>2</sub> Cl <sub>2</sub>	— <sup>e</sup>	0.56	1.00 <sup>c</sup>

<sup>a</sup> Conditions: 0.55–1.0 mM solution with 0.10 M (*n*-Bu<sub>4</sub>N)(ClO<sub>4</sub>) as the supporting electrolyte. <sup>b</sup> All of the potentials are given vs the ferrocene/ferrocenium redox couple as an internal standard. <sup>c</sup> Irreversible anodic peak. <sup>d</sup> Oxidation peaks were not observed <sup>e</sup> Reduction peaks were not observed.

of  $\pi$ -conjugated molecules. The parent **1** showed two reversible one-electron reduction waves in THF.<sup>24</sup> Moreover, chemically generated dianionic species were transformed into bisfulvalene dianions.<sup>25</sup> To evaluate the electronic properties of the new acceptors **2** and **3** and donors **4a** and **5**, cyclic voltammetry measurements were carried out (Table 1).

Parent **1** in CH<sub>2</sub>Cl<sub>2</sub> displayed only one reversible one-electron reduction wave, at  $E_{1/2} = -2.21$  V under our experimental conditions. On the other hand, **2** in 1,1,2,2-tetrachloroethane showed a reversible one-electron reduction wave at  $E_{1/2} = -1.70$  V. The use of 1,1,2,2-tetrachloroethane instead of CH<sub>2</sub>Cl<sub>2</sub> was necessary because of the low solubility of **2**. In 1,1,2,2-tetrachloroethane, **3** also accepts an electron at the same potential ( $E_{1/2} = -1.70$  V). No indications of further reduction or oxidation were observed for either acceptor. The difference in  $E_{1/2}$  values demonstrates the higher electron-accepting abilities of **2** and **3** compared to **1**, in qualitative agreement with the LUMO levels estimated from the theoretical study ( $-2.00$  eV for **1**,  $-2.97$  eV for **3**, and  $-3.20$  eV for **2**).<sup>26</sup>

In the case of **4a** in CH<sub>2</sub>Cl<sub>2</sub>, an irreversible oxidation process at  $E_{\text{pa}} = 0.30$  V that was subsequently subjected to further oxidations was observed. On the other hand, **5** in CH<sub>2</sub>Cl<sub>2</sub> showed a reversible one-electron oxidation wave at  $E_{\text{pa}} = 0.56$  V and an irreversible wave corresponding to further oxidation. Comparison of the first oxidation potentials of the [12]DBAs with electron-donating groups indicates that the electron-donating ability of **4a** is stronger than that of **5**, in agreement with the order of the theoretically calculated HOMO levels ( $-4.47$  eV for **5** and  $-4.35$  eV for **4a**).

The potentials of the donor- and acceptor-substituted [12]DBAs were also compared with those of common organic donors and acceptors. Apparently, the electron-accepting abilities of **2** and **3** are lower than those of fullerene C<sub>60</sub>,<sup>27</sup> perylene diimide,<sup>28</sup> perfluoropentacene,<sup>29</sup> and tetracyanoquinodimethane (TCNQ),<sup>30</sup> whereas **4a** exhibits a high

electron-donating ability comparable to those of triarylamine<sup>31</sup> and tetrathiafulvalene.<sup>32</sup>

**3. Crystal Structure Analyses. a. Packing Diagrams for [12]DBAs.** In general, crystal structures of planar aromatic molecules (without functional groups) are classified into four different types, as proposed by Desiraju and Gavezzotti:<sup>33</sup> herringbone, sandwich herringbone,  $\beta$ , and  $\gamma$ . Crystal structures are determined by (1) the balance between maximizing the dispersion forces and minimizing repulsive forces and (2) various intermolecular directional forces, such as hydrogen-bonding interactions. Previously, two types of crystal structures were reported for the [12]DBA derivatives. The parent **1** was reported to show a herringbone structure, reflecting weak intermolecular  $\pi$ - $\pi$  interactions.<sup>34</sup> Recently, Hisaki, Miyata, and co-workers<sup>35</sup> reported the perfect face-to-face 1D columnar structure of a tricarboxy-substituted [12]DBA, which was maintained by hydrogen-bonding interactions between the carboxy groups and the dimethyl sulfoxide solvent molecules. In order to clarify the effect of substituents on the packing structure, single-crystal X-ray structural analyses of **2**, **3**, and **4b** were undertaken. These molecules adopt characteristic packing diagrams, including a perfect 2D sheet structure, depending on the nature of the functional groups on the  $\pi$  system.

**b. Packing Diagram for Tricyano[12]DBA 2.** Cyano substitution on an aromatic ring has been used for the construction of superstructures by CN $\cdots$ H hydrogen-bonding interactions.<sup>36</sup> Not surprisingly, the molecules of compound **2** pack to form 2D sheets via hydrogen-bonding interactions between the nitrogen atoms of the cyano groups on one molecule and hydrogen atoms attached to the benzene rings of adjacent molecules (Figure 3a,b). The N $\cdots$ H distances range from 2.47 to 2.85 Å, corresponding to the typical CN $\cdots$ H hydrogen-bonding distance.<sup>36</sup> Though there are no significant directional intersheet interactions (Figure 3c), the average distance between adjacent 2D sheets is 3.2 Å, which is shorter than the typical  $\pi$ - $\pi$  interaction distance.

**c. Packing Diagram for Dodecafluoro[12]DBA 3.** The analysis of **3** showed a columnar packing structure in which each molecule is tilted with respect to the main axis of the column (Figure 4a,b). According to the Desiraju–Gavezzotti scheme, this structure is classified as a  $\beta$  structure. In the molecular column, one of the tetrafluorobenzene rings of **3** is aligned face-to-face with the center of an adjacent [12]annulene ring, while the other two tetrafluorobenzene rings do not overlap with their top and bottom neighbors (Figure 4c). The observed positional relationships of the adjacent molecules can be ascribed to intermolecular electrostatic interactions.<sup>14b</sup> In fact, natural-population analysis based on B3LYP/6-31G\* calculations gave high partial positive charges (0.32 to 0.40) for carbon atoms attached to the electronegative fluorine atoms

(24) Ferrara, J. D.; Tanaka, A. A.; Fierro, C.; Tessier-Youngs, C. A.; Youngs, W. J. *Organometallics* **1989**, *8*, 2089–2098.

(25) Malaba, D.; Djebli, A.; Chen, L.; Zarate, E. A.; Tessier, C. A.; Youngs, W. J. *Organometallics* **1993**, *12*, 1266–1276.

(26) Though both **2** and **3** were reduced at the same potential ( $-1.70$  V) in the electrochemical measurements, the LUMO of **2** is lower in energy than that of **3**. One of the plausible reasons for this discrepancy is the difference in the stabilities of their anionic species in solution.

(27) Keshavarz-K, M.; Knight, B.; Srdanov, G.; Wudl, F. *J. Am. Chem. Soc.* **1995**, *117*, 11371–11372.

(28) Pasaogullari, N.; Icil, H.; Demuth, M. *Dyes Pigm.* **2006**, *69*, 118–127.

(29) Sakamoto, Y.; Suzuki, T.; Kobayashi, M.; Gao, Y.; Fukai, Y.; Inoue, Y.; Sato, F.; Tokito, S. *J. Am. Chem. Soc.* **2004**, *126*, 8138–8140.

(30) Gross-Lannert, R.; Kaim, W.; Olbrich-Deussner, B. *Inorg. Chem.* **1990**, *29*, 5046–5053.

(31) Steckhan, E. *Top. Curr. Chem.* **1987**, *142*, 1–69.

(32) Morita, Y.; Miyazaki, E.; Fukui, K.; Maki, S.; Nakasuji, K. *Bull. Chem. Soc. Jpn.* **2005**, *78*, 2014–2018.

(33) Desiraju, G. R.; Gavezzotti, A. *J. Chem. Soc., Chem. Commun.* **1989**, 621–623.

(34) Irngartinger, H.; Leiserowitz, L.; Schmidt, G. M. *J. Chem. Ber.* **1970**, *103*, 1119–1131.

(35) Hisaki, I.; Sakamoto, Y.; Shigemitsu, H.; Tohno, N.; Miyata, M.; Seki, S.; Saeki, A.; Tagawa, S. *Chem.—Eur. J.* **2008**, *14*, 4178–4187.

(36) Yokoyama, T.; Yokoyama, S.; Kamikado, T.; Okuno, Y.; Mashiko, S. *Nature* **2001**, *413*, 619–621.

(37) (a) Meyer, E. A.; Castellano, R. K.; Diederich, F. *Angew. Chem., Int. Ed.* **2003**, *42*, 1210–1250. (b) Hunter, C. A.; Lawson, K. R.; Perkins, J.; Urch, C. J. *J. Chem. Soc., Perkin Trans. 2* **2001**, 651–669.

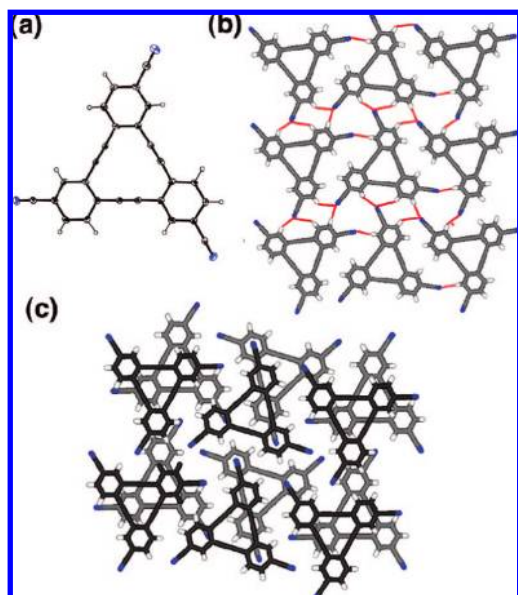


**Figure 3.** Single-crystal X-ray analysis of **2**. (a) ORTEP diagram (50% probability level). (b) Packing structure. The red lines connecting nitrogen atoms (blue) and hydrogen atoms (white) highlight the CN $\cdots$ H hydrogen-bonding interactions. (c) Positional relationship between the molecular sheets. Molecules forming the upper layer are drawn darker than those in the lower layer.

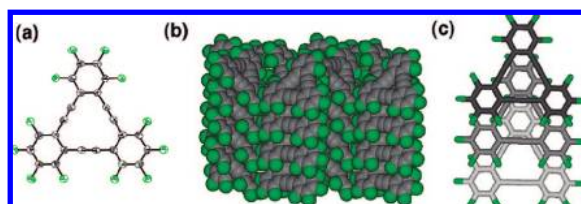


**Figure 4.** Single-crystal X-ray analysis of **3**. (a) ORTEP diagram (50% probability level). (b) Packing structure. (c) Positional relationship between adjacent molecules in a molecular column. The upper molecules are drawn darker than the lower molecules.

but negative or very weakly positive charges ( $-0.14$  to  $0.03$ ) for carbons in the [12]annulene ring. Consequently, we assume that electrostatic repulsions between tetrafluorobenzene rings and attractive forces between tetrafluorobenzene and [12]annulene rings led to the formation of the tilted-stack structure.

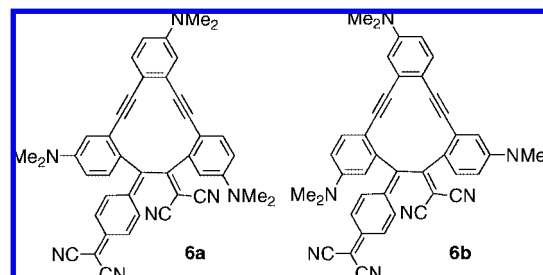
**d. Packing Diagram for Tris(dibutylamino)[12]DBA 4b.** The analysis of **4b** revealed a 2D sheet structure consisting of 1D tapes (Figure 5a,b) in which the [12]DBA units roughly align within the plane. The butyl groups occupy the spaces between the  $\pi$  cores both within a plane and between planes, indicating that van der Waals interactions play a major role in this packing diagram. In regard to intersheet interactions, two of the benzene rings of each **4b** molecule show short distances ( $3.47$  to  $3.80$  Å) with respect to rings of neighboring molecules (one above and one below), as shown in Figure 5c.

**4. Formation of Charge-Transfer Complexes between [12]DBAs.** In general, for small  $\pi$  systems without  $\pi$ – $\pi$  interactions significant enough to form a stacked structure, two interactions can be used to achieve a face-to-face packing pattern: quadrupole–quadrupole interactions between a perfluorobenzene ring and a benzene ring and charge-transfer

interactions between a donor and an acceptor.<sup>37</sup> Unusual properties of perfluoroaromatic compounds were discovered five decades ago in a study of the formation of a crystal from a mixture of perfluorobenzene and benzene.<sup>38</sup> The formation of an alternating, perfectly face-to-face packing structure has been ascribed to favorable quadrupole–quadrupole interactions and reduction of unfavorable electrostatic repulsions.<sup>39</sup> This type of interaction has been successfully used for the construction of not only superstructures in crystals but also supramolecules.<sup>40</sup> The other important interaction is the charge-transfer interaction. The simplest charge-transfer complex was discovered four decades ago in a study of a mixture of perfluorobenzene and *N,N*-dimethylaniline;<sup>41</sup> this complex adopts a slightly displaced parallel-packing mode in crystals.<sup>42</sup> In both cases, the donor and acceptor molecules favor the formation of 1D columnar structures with alternating alignment. On the basis of these precedents, we examined the formation of cocrystals between dodecafluoro[12]DBA **3** and parent [12]DBA **1** and of charge-transfer complexes between the donor **4a** and the acceptors **2** and **3**.<sup>43</sup> However, in a systematic investigation of the mixtures, we obtained cocrystals only for **4a** and **3**; slow evaporation of the solvent from a mixture of **3** and **4a** in  $\text{CHCl}_3$  formed red-colored crystals suitable for X-ray analysis. Nevertheless, single-crystal X-ray structural analysis turned out to be challenging because of the exotic packing diagram. However, in the unit cell, there are two different trimers: trimer A consists of one molecule of **3** and two molecules of **4a** (acceptor/donor ratio of 1:2), and trimer B contains two molecules of **3** and one molecule of **4a** (acceptor/donor ratio of 2:1) (Figure 6a). The unit cell also contains two chloroform molecules (Figure 6b) and overall is very large ( $V = 6721$  Å<sup>3</sup>).

Each [12]DBA adopts displaced parallel packing, with one C–C bond of one benzene ring located above the center of

- (38) Patrick, C. R.; Prosser, G. S. *Nature* **1960**, *187*, 1021.  
 (39) Williams, J. H.; Cockcroft, J. K.; Fitch, A. N. *Angew. Chem., Int. Ed. Engl.* **1992**, *31*, 1655–1657.  
 (40) (a) Coates, G. W.; Dunn, A. R.; Henling, L. M.; Ziller, J. W.; Lobkovsky, E. B.; Grubbs, R. H. *J. Am. Chem. Soc.* **1998**, *120*, 3641–3649. (b) Weck, M.; Dunn, A. R.; Matsumoto, K.; Coates, G. W.; Lobkovsky, E. B.; Grubbs, R. H. *Angew. Chem., Int. Ed.* **1999**, *38*, 2741–2745. (c) Ponzini, F.; Zagha, R.; Hardcastle, K.; Siegel, J. S. *Angew. Chem., Int. Ed.* **2000**, *39*, 2323–2325. (d) Shu, L.; Mayor, M. *Chem. Commun.* **2006**, 4134–4136.  
 (41) Beaumont, T. G.; Davis, K. M. C. *Nature* **1968**, *218*, 865.  
 (42) Dahl, T. *Acta Crystallogr.* **1977**, *B33*, 3021–3024.  
 (43) We also attempted the preparation of charge-transfer complexes of donor **4a** with common acceptors such as TCNQ. However, treatment of **4a** with TCNQ afforded the covalently bonded products **6a** and **6b** via [2 + 2] cycloaddition followed by electrocyclic ring opening. Similar reactions were employed by Diederich and co-workers<sup>44</sup> to prepare compounds containing charge-transfer chromophores.



- (44) Kivala, M.; Boudon, C.; Gisselbrecht, J.-P.; Seiler, P.; Gross, M.; Diederich, F. *Chem. Commun.* **2007**, 4731–4733.  
 (45) Gung, B. W.; Amicangelo, J. C. *J. Org. Chem.* **2006**, *71*, 9261–9270.  
 (46) Rowland, R. S.; Taylor, R. *J. Phys. Chem.* **1996**, *100*, 7384–7391.

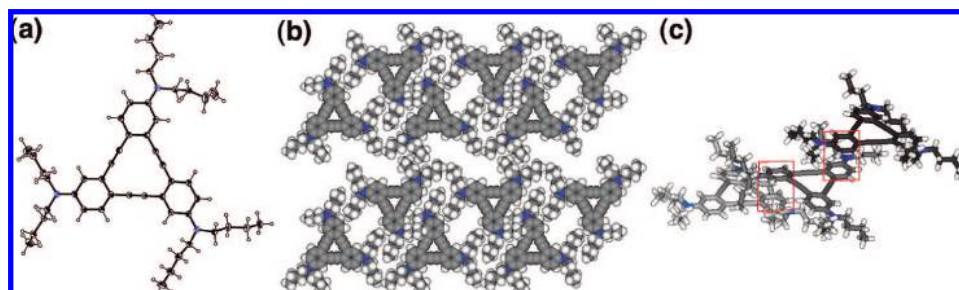


**Figure 5.** Single-crystal X-ray analysis of **4b**. (a) ORTEP diagram (50% probability level). (b) Packing structure. (c) Positional relationships of the adjacent molecules between molecular sheets. The upper molecules are drawn darker than the lower molecules. The red squares highlight the position of short interring distances.

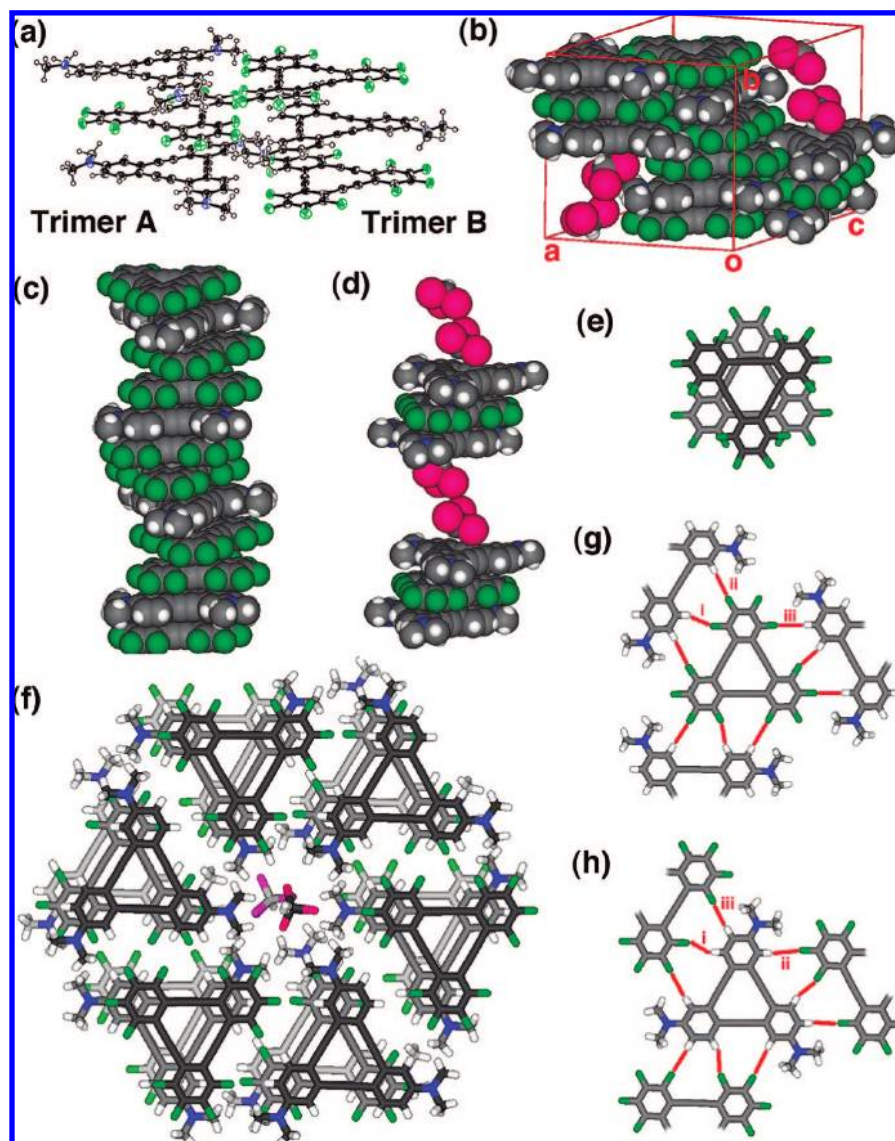


**Figure 6.** Single-crystal X-ray analysis of the charge-transfer complex **4a·3**. (a) ORTEP diagrams (50% probability level) of layered trimers A and B. (b) Unit cell structure. The pink-colored atoms are chlorine atoms of chloroform. (c) Columnar structure in the unit cell *b* direction, consisting of four units of trimer B. (d) Structure in the unit cell *b* direction, consisting of two units of trimer A and four molecules of chloroform. (e) Positional relationship between adjacent molecules of **3** in the *b* direction. The upper molecule is drawn darker than the lower one. (f) Triple-layered rosette structure in the crystal. The color gradation shades the upper molecules darker than the lower molecules. (g, h) Partial structures within the molecular sheet. The red lines highlight places where short CH...F contacts were observed.

the adjacent ring, instead of a perfect sandwich configuration. This geometry is similar to that observed for the charge-transfer complex of perfluorobenzene and *N,N*-dimethylaniline.<sup>42</sup> In addition, a theoretical study has indicated that

the stable form of that charge-transfer complex is a slightly displaced parallel-packing mode.<sup>45</sup> Thus, the observed structure in trimers A and B can be regarded as arising from the typical packing pattern for the charge-transfer complex of

perfluorobenzene and dimethylaniline. However, the cocrystal of **3** and **4a** consists of 1:2 and 2:1 rather than 1:1 complexes, even though the net ratio of **3** to **4a** is 1:1. The formation of the sandwich trimers may be ascribed to their height, which provides sufficient space to accommodate the two chloroform molecules occupying the void formed as a result of the difference in the bulkiness of the substituents of **3** and **4a** (Figure 6b). As a result, one of the trimers, B, forms a columnar assembly along the unit cell *b* direction (Figure 6c). At the contact between the trimer units, the orientation of the adjacent **3** molecules is antiparallel in order to avoid the electrostatic repulsion between fluorinated rings and to maximize close-packing (Figure 6e). On the other hand, trimer A does not form a 1D column in the *b* direction; two chloroform molecules occupy the space between the trimers (Figure 6d). The absence of columnar assembly can be ascribed to the unfavorable interactions between the donor **4a** molecules that would arise at the contacts between trimer A units.

More significantly, all of the trimers align in the *ac* plane to form a 2D rosette pattern (Figure 6f). The formation of this particular packing structure is attributed not only to the triangular shapes of **3** and **4a**, which are favorable for packing them into a 2D hexagonal pattern, but also to the side-by-side intermolecular interactions between adjacent triangular cores. Indeed, relatively short interatomic distances are found between the fluorine atoms of **3** and the hydrogen atoms of **4a**; the average CH...F distances are 2.49, 2.82, and 2.73 Å, respectively, for contacts (i), (ii), and (iii) shown in Figure 6g,h. In particular, the average distance for (i) is shorter than the sum of the van der Waals radii of the two nuclei (2.56 Å),<sup>46</sup> indicating the existence of a favorable CH...F interaction.<sup>47</sup> Therefore, the 2D rosette structure consisting of the two types of trimers is formed by (1) intermolecular charge-transfer interactions between the donor **4a** and the acceptor **3** along the *b* direction and (2) the favorable packing geometry due to the triangular shapes together with lateral CH...F hydrogen bonding. To our knowledge, this unique structural feature has not been reported previously.

## Summary

In summary, donors and acceptors based on [12]DBA, namely, the donors tricyano[12]DBA **2** and perfluoro[12]DBA **3** and the tris(dialkylamino)[12]DBA acceptors **4a–d**, were synthesized and their electronic properties characterized by electronic absorption and emission spectra and redox mea-

surements. The crystal structures of **2**, **3**, and **4b** were determined by single-crystal X-ray analyses, which revealed the formation of distinct packing patterns, such as the perfect 2D sheet structure of **2** arising from intraplane CN...H interactions. In addition, in crystals of the charge-transfer complex **3·4a**, the combination of charge-transfer interactions, the characteristic triangular molecular shapes, and intermolecular CH...F interactions results in the formation of a 2D bimolecular rosette structure using two different molecular trimers as building blocks. The present study provides some new insights regarding methods for controlling the spatial arrangement of  $\pi$ -conjugated molecules, which is crucial for optoelectronic applications.

**Acknowledgment.** This work was supported by a Grant-in-Aid for Scientific Research from the Ministry of Education, Culture, Sports, Science, and Technology of Japan. The authors thank Prof. M. Miyata and Dr. I. Hisaki (both of Osaka University) and Dr. Y. Matsuo (ERATO, Nakamura Functional Carbon Cluster Project) for their help with single-crystal X-ray analysis.

**Note Added after ASAP Publication.** After this paper was published ASAP September 25, 2008, production errors in the next-to-last sentence of the second paragraph, including reference numbering, were corrected. The corrected version was published October 1, 2008.

**Supporting Information Available:** Synthetic procedures and experimental and computational procedures; characterization data for [12]DBA derivatives **2**, **3**, and **4a–d**; calculated HOMO/LUMO levels of triphenylene derivatives; crystallographic data for **2**, **3**, **4b**, and the charge-transfer complex **4a·3** (CIF); cyclic voltammograms and electronic absorption and emission spectra of **1**, **2**, **3**, **4a**, and **5**; NMR spectra of all of the new compounds; and optimized structures of the model compounds. This material is available free of charge via the Internet at <http://pubs.acs.org>.

JA804604Y

- (47) (a) Dahl, T. *Acta Crystallogr.* **1990**, *B46*, 283–288. (b) Collings, J. C.; Roscoe, K. P.; Thomas, R. L.; Batsanov, A. S.; Stimson, L. M.; Howard, J. A. K.; Marder, T. B. *New J. Chem.* **2001**, *25*, 1410–1417. (c) Batsanov, A. S.; Collings, J. C.; Howard, J. A. K.; Marder, T. B. *Acta Crystallogr.* **2001**, *E57*, o950–o952.